ORIGINAL ARTICLE

Thermal characteristic analysis of ball screw feed drive system based on finite difference method considering the moving heat source

Yang Li[1] · Wenming Wei[1] · Dongxu Su[1] · Wenwu Wu[2] · Jun Zhang[1] · Wanhua Zhao[1]

Abstract

The thermal characteristic of the ball screw feed drive system has great influence on machining accuracy as its thermal deformation would induce the positioning deviation. In this paper, finite difference method was applied to simulate the temperature distribution and thermal growth of the ball screw feed drive system under various working conditions. When simulating, the nut was considered a moving heat source, and the boundary conditions were optimized based on response surface methodology. By comparing the simulation results with the testing data, it was verified that the accuracy of the simulation could be improved by using the proposed method.

Keywords Finite difference method · Ball screw feed drive system · Thermal characteristic · Moving heat source · Boundary condition optimization

1 Introduction

The ball screw is the widely used drive system in machine tool due to its high efficiency, good stiffness, and long lifetime. However, when it is moving rapidly for high-speed manufacturing, a great deal of heat is generated at bearings and the nut because of the friction, which could lead to the temperature rise and thermal deformation [1, 2]. Furthermore, the thermal deformation of the ball screw feed drive system would bring about the positioning deviation and finally result in deterioration of manufacturing accuracy [3]. Therefore, scholars and engineers devote to study the thermal characteristics of the ball screw feed drive system and reduce the thermal error [2, 4–6].

Numerical simulation and practical testing are the two most popular ways to investigate how the heat is transferred in the ball screw and how the shaft is deformed. Finite element method (FEM) is one of the most commonly used methods to simulate the thermal characteristic of the ball screw feed drive system numerically. Li [7] and Min [8] calculated the heat generation and boundary conditions mathematically at first. Then, they investigated the temperature fields and thermal deformations of the ball screw feed drive systems based on the FEM model. Oyanguren [9] built two 3-D FEM models of the double-nut ball screw. One was the heat transfer model which was used to predict the transient temperature. The other was the mechanical model which was applied to simulate thermal expansions, stresses, and contact forces. In Li's work [10], FEM was integrated with the Monte Carlo method. Then, the heat flow rates, the temperature distribution, and the thermal errors of ball screw feed drive systems were predicted. In addition, Wu [11] developed a simplified FEM model of the ball screw feed drive system. The temperature rise after long-term movement of the working table was measured and used to determine the strength of the frictional heat source by inverse analysis, which was then applied to calculate the thermal error based on the FEM model. At last, the calculation results were compared with testing data to verify the correctness of the model. It is easier and costless for scholars to know the thermal characteristics of the ball screw feed drive system by using the finite element method. However, some assumptions were made to perform the thermal analysis based on FEM, and the computed value of heat sources and boundary conditions for the numerical simulation

✉ Yang Li
liyangxx@xjtu.edu.cn

1 State Key Laboratory for Manufacturing Systems Engineering, Xi'an Jiaotong University, Xi'an 710049, China

2 Key Laboratory of NC Machine Tools and Integrated Manufacturing Equipment of the Education Ministry & Key Lab of Manufacturing Equipment of Shaanxi Province, Xi'an University of Technology, Xi'an, Shaanxi, China

⌀ Springer

are different with the practical working conditions at some degree. Therefore, the simulation accuracy could be affected [11, 12].

By testing, thermal characteristics under practical working conditions can be obtained. Shi and Yang [13–15] conducted several experiments on a CNC precision boring machine. The relationships between the thermal error and the axial thermal expansion as well as temperature of dual ball screw feed drive system were explored. It was found out that the thermal error along the axis was nearly linear, but it was nonlinear with working time. However, the working conditions are various in practical. It is cumbersome to measure the temperature changings and thermal error deformation as the ball screw feed drive system is running at different feeding speed and in different ranges, and it is difficult to obtain the data sometimes. For example, the temperature of the shaft is hard to collect by using contact temperature sensors when the shaft is rotating. Although, it is possible to obtain the temperature of the shaft of the ball screw feed drive system by using the thermal infrared imager, the accuracy of the testing is limited, and the cost of the testing is high.

Therefore, a novel finite difference model is established in this paper to study the thermal characteristics of the ball screw feed drive system. In the model, the nut is considered a moving heat source, and the boundary conditions when the nut is moving in different ranges at different speeds are applied for simulation, which could help to improve the simulation accuracy. Based on the model, the temperature of shaft and positioning deviations under various working conditions are simulated. Finally, the simulation results are verified with the experiment data.

2 Thermal model of the ball screw feed drive system based on finite difference methodology

2.1 Heat sources s of the ball screw feed drive system

As shown in Fig. 1, the ball screw feed drive system is always simplified as the one-dimensional model.

In the model, the motor drives the ball screw to rotate. The motor is connected to the screw by the shaft coupling, and it is assumed that there is little heat transferred from the motor to the ball screw. Therefore, the front bearing, the nut, and
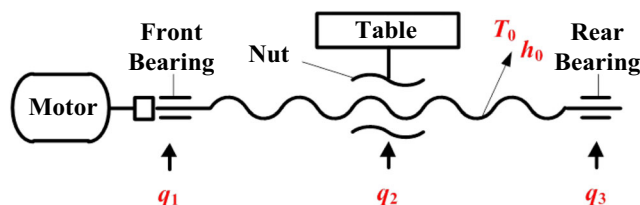

Fig. 1 Simplified model of the ball screw feed drive system

the rear bearing are considered as the heat sources of the ball screw feed drive system. The heat fluxes transferred from these heat sources to the system are named as q_1, q_2, and q_3, respectively. In addition, a part of heat is dissipated through heat convection, and the heat convection coefficient is h_0. The initial temperature distribution is considered uniform, and the value is T_0.

The heat generated from bearings is labeled as Q_b, which can be computed as follows [16, 17].

$$Q_b = 1.047 \times 10^{-4} n_b M_b \tag{1}$$

$$M_b = M_{b1} + M_{b2} \tag{2}$$

$$M_{b1} = f_{b1} \cdot P_{b1} \cdot d_{bm} \tag{3}$$

$$M_{b2} = \begin{cases} 10^{-7} f_{b2} (v_b n_b)^{\frac{2}{3}} d_{bm}^3 & v_b n_b \geq 2000 \\ 160 \times 10^{-7} f_2 d_{bm}^3 & v_b n_b < 2000 \end{cases} \tag{4}$$

where, n_b is the speed of the bearing, r/min. M_{b1} and M_{b2} represent the friction torques related to the external load and the viscous friction, respectively, M mm. f_{b1} and f_{b2} are coefficients which are determined by the type, the load, and the lubrication condition of bearings. d_{bm} is the pitch diameter, m. v_b is the kinematic viscosity of the lubricant, cSt.

P_{b1} is dependent on the force of the bearing.

$$P_{b1} = a F_{br} + b F_{ba} \tag{5}$$

where, a and b are the coefficients. F_{ba} and F_{br} are the axial and radial force of bearings, N.

Meantime, the heat generated due to the friction between the nut and the ball screw can be computed according to Eq. (6).

$$Q_{nut} = 0.12 \pi n_{nut} M_{nut} \tag{6}$$

$$M_{nut} = M_{nut\_a} + M_{nut\_b} \tag{7}$$

$$M_{nut\_a} = \frac{F_{nut\_a} \cdot P_h}{2\pi\eta} (1-\eta) \tag{8}$$

$$M_{nut\_b} = \frac{F_{nut\_b} \cdot P_h}{2\pi\eta} (1-\eta^2) \tag{9}$$

where, n_{nut} is the rotational speed of the ball screw, r/min; M_{nut_a} is the torque which is used to overcome the axial force and cutting force, N/m; M_{nut_b} is the torque which is related to the preload of the nut, N/m; F_{nut_a} and F_{nut_b} is the axial force and the preload, respectively, N; P_h is the lead of the screw, m; η is the transmission efficiency (0.95~0.98).

Then heat flux q_1, q_2, and q_3 in the model can be obtained according to the following equations.

$$q = \frac{Q}{A} \tag{10}$$

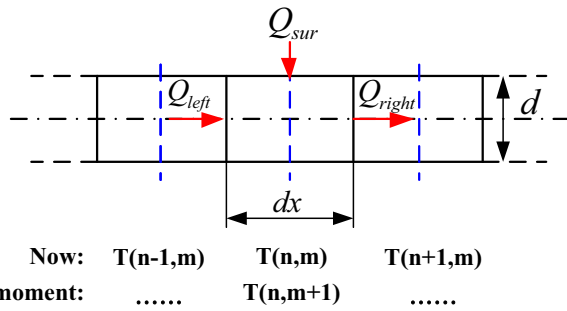where, Q is the heat generated from bearings or the nut, W; A is the area, m^2.

Fig. 2 Heat transfer of the element in the middle of the ball screw

2.2 Heat dissipation of the ball screw feed drive system

In this paper, heat convection is considered the main way of heat dissipation, and the heat radiation is neglected. When the feed drive system is running, the heat is transferred by forced convection. Otherwise, it is considered that the heat is dissipated by the free convection. The convection heat transfer coefficient h can be computed as follows.

$$h = \frac{Nu \cdot \lambda f}{L} \tag{11}$$

where, N_u is the Nusselt number; λ_f is the heat conductivity of the fluid, W/(m °C), L is the feature size, m.

1) Free convection heat transfer coefficient

For lots of circumstances, the free convection heat transfer coefficient can be calculated according to Eq. (11), in which Nusselt number N_u is represented as:

$$N_u = C(Gr \cdot \text{Pr})^{\frac{1}{4}} \tag{12}$$

where, C is the constant. Pr is Prandtl number. Gr is Grashof number, which can be obtained based on the following equation.

$$Gr = \frac{g \cdot \beta \cdot L^3 \cdot \Delta T}{\upsilon^2} \tag{13}$$

where, g is the acceleration of gravity, m/s². β is the volume coefficient of expansion, 1/K. ΔT is the temperature differences between the parts of the feed drive system and the fluid. υ is the kinematic viscosity of the fluid, m²/s.

In summary, the free convection heat transfer coefficients between parts of the feed drive system and the fluid (normally the air) can be obtained according to the following equation.

$$h = \frac{C \cdot \lambda}{L} \left(\frac{g \beta L^3 \Delta T}{\upsilon^2} \cdot \text{Pr} \right)^{\frac{1}{4}} \tag{14}$$

2) Forced convection heat transfer coefficient

Different with the free convection, the Nusselt number of forced convection can be obtained based on the following equation.

$$N_u = 0.133 Re^{\frac{2}{3}} \text{Pr}^{\frac{1}{4}} \tag{15}$$

where, Re is the Reynolds number which is represented as

$$Re = \frac{\pi n_{nut} d^2}{60 \upsilon} \tag{16}$$

where, d is the diameter of the ball screw, m.

Finally, the equation for computing the forced convection heat transfer coefficient can be derived.

$$h = \frac{0.133 \lambda_f \left(\frac{\pi n_{nut} d^2}{60 \upsilon} \right)^{\frac{2}{3}} \text{Pr}^{\frac{1}{4}}}{L} \tag{17}$$

2.3 Heat transfer model of the ball screw feed drive system under various working conditions based on FDM

Finite difference method (FDM), finite element method (FEM), finite analytic method (FAM), and finite volume method (FVM) are widely used numerical analysis methods. Based on FEM, some commercial softwares, such as ANSYS, were emerged and applied for simulation in the field of heat transfer. Although the simulation stability is commonly good, the accuracy is highly dependent on the boundary conditions. Unfortunately, the working conditions of the ball screw feed drive system are complex in practical. The nut is always moving in different ranges under different speeds for different periods of time, and the nut becomes a moving heat source. In other words, working conditions are complicated and hard to be determined for finite element analysis. By contrast, FDM is suitable for learning the heat transfer in the object of simple geometry, and the time for numerical simulation is relatively short. Therefore, FDM is applied to establish the heat transfer
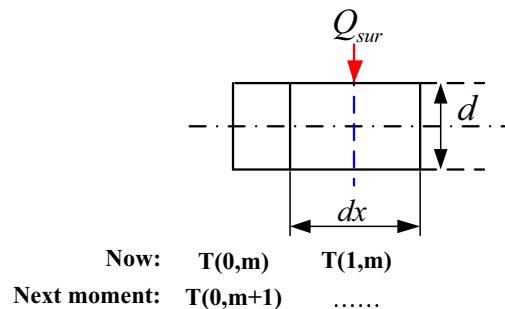

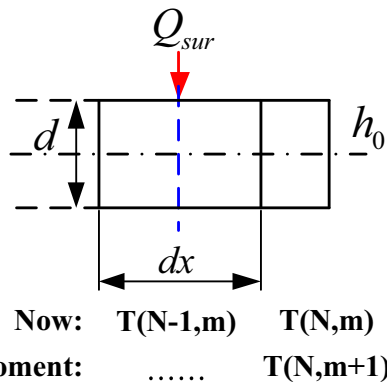**Fig. 3** Heat transfer of the element at the left end of the ball screw (near front bearing)

Fig. 4 Heat transfer of the element at the left end of the ball screw (near rear bearing)

model of the ball screw system in this paper in which the moving heat source is considered as well.

Supposing that the length of the screw is L, and it is composed of N elements with length of dx. The total time for the heat transfer is supposed as t, and it is divided into M elements of which the duration time is dt. It is considered that there is a node in the middle of each element. The temperature of the node is represented as the average temperature of the element. For example, $T(n,m)$ is considered the average temperature of the nth element at moment m. $T(n-1,m)$ and $T(n+1,m)$ are the temperatures of elements next to the nth element at the same time. $T(n,m+1)$ is the temperature of the nth element at the moment $m+1$. The heat transfer model of the ball screw feed drive system based on FDM is showed in Fig. 2. Q_{sur} is the heat transferred between the nth element and surroundings at moment t. x is related to the position of the nut. d is the equivalent diameter of the ball screw.

Take the nth element for example, the heat flowing into it from the left element Q_{left} at moment m can be computed based on the Fourier law.

$$Q_{left} = -\lambda \frac{T(n,m)-T(n-1,m)}{dx} \frac{\pi d^2}{4} \tag{18}$$

where, λ is the heat conductivity coefficient, W m^{-1} K^{-1}.

Similarly, the heat flowing into the nth element from right Q_{right} at moment m is

$$Q_{right} = -\lambda \frac{T(n+1,m)-T(n,m)}{dx} \frac{\pi d^2}{4} \tag{19}$$

The heat transferred from surroundings is labeled as Q_{sur}.

$$Q_{sur} = q(x)\pi d \cdot dx \tag{20}$$

According to the conservation law, we know that

$$Q_{left} + Q_{sur} + \dot{Q} = Q_{right} + Q_{in} \tag{21}$$

where, $\dot{Q}$ and Q_{in} are the heat generated in the system and the increment of internal energy, respectively.

In this case,

$$\dot{Q} = 0 \tag{22}$$

$$Q_{in} = \rho c \frac{T(n,m+1)-T(n,m)}{dt} dx \frac{\pi d^2}{4} \tag{23}$$

Substituting Eq. (22) and Eq. (23) into Eq. (21), then

$$T(n,m+1) = \frac{\lambda}{\rho c} \frac{dt}{dx^2} [T(n-1,m) + T(n+1,m)]$$
$$+ \left(1-2\frac{\lambda}{\rho c}\frac{dt}{dx^2}\right)T(n,m) + \frac{4dt}{\rho cd}q(x) \tag{24}$$

Supposing that,

$$\gamma = \frac{\lambda}{\rho c}\frac{dt}{dx^2}$$

$$\beta = \frac{4dt}{\rho cd}$$

Then Eq. (24) can be changed into Eq. (25).

$$T(n,m+1) = \gamma[T(n-1,m) + T(n+1,m)]$$
$$+ (1-2\gamma)T(n,m) + \beta q(x) \tag{25}$$

The left end of the ball screw is connected to the motor by coupling, it assumed that there is little heat transferred into screw from left. The heat transfer model of ball screw at the left end is shown in Fig. 3, in which $T(0,m)$ is the average temperature of the element at the left end at moment m. The

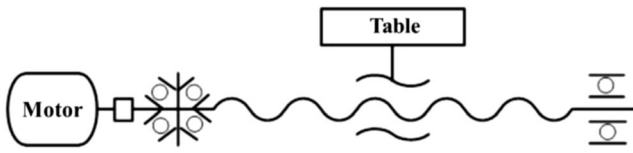**Fig. 5** The nut position when it is moving in a range of the ball screw
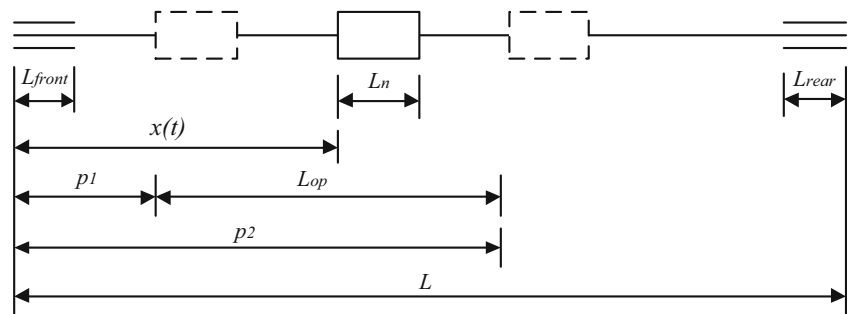
Fig. 6 One of the installation methods for the ball screw feed drive system

relationship between $T(0, m)$, $T(0, m + 1)$, and $T(1,m)$ is shown in Eq. (26).

$$T(0, m + 1) = (1-\gamma)T(0, m) + \gamma T(1, m) + \beta q(x) \qquad (26)$$

Figure 4 shows the heat transfer in the element at the right end. As the right end is exposed to the air, the heat is transfer by convection. The convection heat transfer coefficient is assumed as h_0. $T(N, m + 1)$ represents the average temperature of the element at the right end at moment $m + 1$, which can be computed according to the following equation (Eq. (27)).

$$T(N, m + 1) = \gamma T(N-1, m) + (1-\gamma)T(N, m)$$
$$+ \frac{\beta d}{4dx} h_0[T_0 - T(N, m)] + \beta q(x) \qquad (27)$$

According to Eq. (25), (26), and (27), Eq. (28) can be derived. Then the temperature of the ball screw at different locations and different moments can be obtained through iterative computing.

$$T(n, m+1) = \begin{cases} (1-\gamma)T(n,m) + \gamma T(1,m) + \beta q(x) & n = 0 \\ \gamma[T(n-1,m) + T(n+1,m)] + (1-2\gamma)T(n,m) + \beta q(x) & 0 < n < N \\ \gamma T(n-1,m) + (1-\gamma)T(n,m) + \frac{\beta d}{4dx} h_0[T_0 - T(n,m)] + \beta q(x) & n = N \end{cases} \qquad (28)$$

where, $q(x)$ is determined by the position of x on the ball screw.

$$q(x) = \begin{cases} q_1 & 0 < x \leq L_{front} \\ q_2 & x(t) \leq x \leq L_n + x(t) \\ q_3 & L - L_{rear} \leq x \leq L \\ -h_0\left[T(n,m) - T_0\right] & elsewhere \end{cases} \qquad (29)$$

Table 1 Parameters of the X-axis ball screw feed drive system

Full length/ mm	Diameter of the shaft/mm	Effective start point/ mm	Effective end point/ mm	Effective moving range/ mm	Length of nut/ mm	Lead of the ball screw/ mm
1800	37	460	1260	800	120	12

Table 2 Material properties of the X-axis ball screw feed drive system

ρ/kg·m^{-3}	E /Gpa	C /J·kg^{-1}·k^{-1}	λ /w·m^{-1}·k^{-1}	α / μm·m^{-1}·k^{-1}
7850	200	448	70	12

where, q_1 and q_3 are the heat flux of the bearings at front and rear end of the ball screw, respectively. Heat flux from the nut to the shaft is q_2. It is assumed that bearings are installed at the very end of the ball screw feed drive system. L_{front} and L_{rear} are the width of bearings at each end, and L_n is the width of the nut. L is the length of the ball screw. $x(t)$ is the location of the nut at moment t. Supposing that the nut is moving from $p1$ to $p2$ at speed of v for a period of time(Fig. 5), then $x(t)$ can be obtained according to Eq. (30).

$$x(t) = \begin{cases} \left[floor\left(\frac{v\cdot t}{L_{op}}\right) + 1\right]\cdot L_{op} - v\cdot t + p_1 & mod\left[floor\left(\frac{v\cdot t}{L_{op}}\right), 2\right] = 1 \\ v\cdot t - floor\left(\frac{v\cdot t}{L_{op}}\right)\cdot L_{op} + p_1 & mod\left[floor\left(\frac{v\cdot t}{L_{op}}\right), 2\right] \neq 1 \end{cases} \qquad (30)$$

where, $L_{op} = p_2 - p_1$ and $p_1 \leq x(t) \leq p_2$.

According to Eq. (28), the temperature and the thermal deformation of the ball screw feed drive system are simulated by using MATLAB. In the finite difference model, the moving heat source is taken into consideration for simulation, and it would help to improve the accuracy of analysis.

2.4 Thermal deformation of the ball screw feed drive system

It is common that the ball screw feed drive system is fixed at one end and supported at the other end (Fig. 6), which means it could expand freely when heated. Based on Eq. (31), the thermal growth of each segment of the ball screw at different moment ($\Delta E(x_i, t_j)$) can be computed.

$$\Delta E(x_i, t_j) = \alpha \cdot \Delta T(i, j) \cdot dx \qquad (31)$$

where, α is the coefficient of linear thermal expansion, K^{-1}. $\Delta T(i, j)$ is the temperature of the ith element at the jth moment. dx is the length of the element.

By summation, the thermal growth of the ball screw feed drive system $E(x_i, t_j)$ at location x_i at moment t_j can be obtained.

$$E(x_i, t_j) = \Delta E(x_i, t_j) + \Delta E(x_{i-1}, t_j) + \ldots$$
$$+ \Delta E(x_i, t_j) \qquad (32)$$

Table 3 The boundary conditions before and after optimization (ambient temperature = 20 °C, feeding rate = 5.4 m/min)

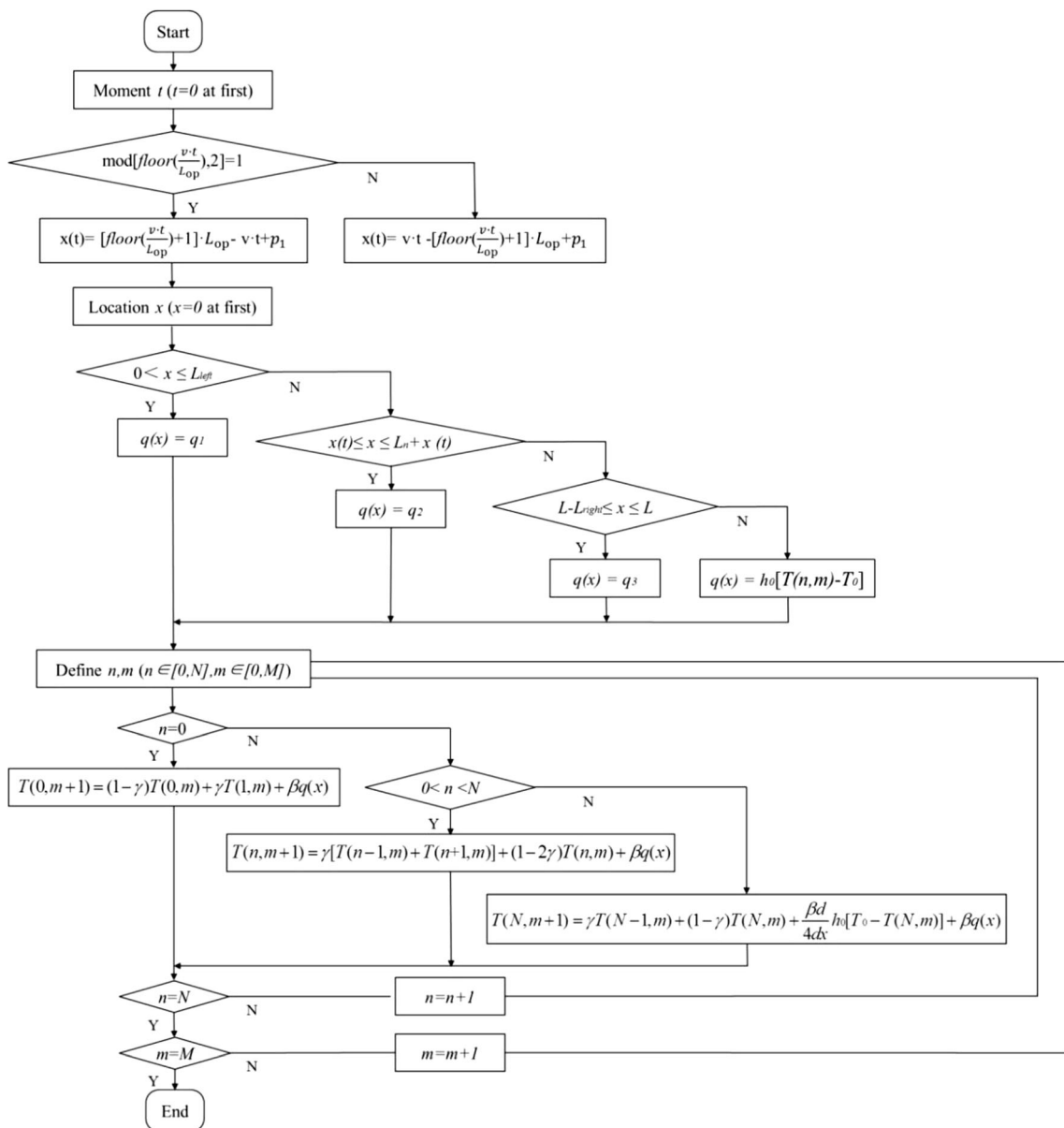|	Heat flux (W/m^2)			Convection heat transfer coefficient ($W/(m^2·K)$)
	x_1	x_2	x_3	x_4
Before optimization	2015	1200	565.2	70
After optimization	1788.6	1027.3	605.7	67.2

Fig. 7 Flow chart of the thermal characteristics simulation process based FDM

3 Thermal characteristic analysis of ball screw feed drive system based on FDM

3.1 Study object

In this paper, *X*-axis of a CNC milling machine (DK-1200) is selected as the study objet to analyze the thermal characteristic of the ball screw feed drive system under different working conditions based on FDM. The ball screw (type 1R40-10B1-FOWC) is manufactured by PMI Company. Some related parameters are shown in Tables 1 and 2. In the table, ρ is density, *E* represents elastic modulus. *C*, λ, and α is specific heat capacity, heat conductivity coefficient, and the coefficient of linear thermal expansion, respectively.

The ball screw is fixed by a pair of angular contact bearings (7006C/DF, contact angle is 15°) at the front end which is near to the motor. At the other end, it is supported by the deep groove ball bearing (61906).

3.2 Boundary condition optimization based on response surface methodology

According to Section 2.1 and 2.2, the generated heat and convection heat transfer coefficient when the nut is moving at 5.4 m/min are calculated. In order to improve the simulation accuracy, these boundary conditions are optimized based on the response surface methodology in this paper.

Response surface methodology was proposed by Box and Wilson in 1951. It is applied for modeling and analysis of problems in which a response of interest is affected by several variables. The second-order model (Eq. (33)) is widely used to optimize the response [18].

Table 4   Working conditions

	A	B
Heat flux of front bearing(W/m^2)	1332.5	1332.5
Heat flux of rear bearing(W/m^2)	1200	1200
Heat flux of the nut(W/m^2)	0	865.2
Convection heat transfer coefficient ($W/(m^2 \cdot K)$)	70	70
Location of the moving heat source *(mm)*	0	466~1073.6

$$Y = f(x) + \varepsilon = \beta_0 + \sum_{i=1}^{k} \beta_i x_i + \sum_{i=1}^{k} \beta_{ii} x_i^2 + \sum_i \sum_j \beta_{ij} x_i x_j + \varepsilon, i < j \quad (33)$$

where, *Y* is the response variable. *f(x)* is the approximation of the response function. x_i represents the independent variable. ε is the error. β_0, β_i, β_{ii}, and β_{ij} are the coefficients which can be determined by the method of least square.

In this paper, heat flux of the front bearing, the rear bearing, and the nut are denoted as x_1, x_2, and x_3. Forced convection heat transfer coefficients of the ball screw is the independent variable x_4. Free convection heat transfer coefficient is assumed as constant (value = 9 $W/(m^2 \cdot K)$). Then, the approximation of the response function f(x_1, x_2, x_3, x_4) can be obtained.

$$f(x_1, x_2 ..., x_4) = \beta_0 + \beta_1 x_1 + \beta_2 x_2 + \beta_3 x_3 + \beta_4 x_4 + \beta_{11} x_1^2 + \beta_{22} x_2^2 + \beta_{33} x_3^2 + \beta_{44} x_4^2 + \beta_{12} x_1 x_2 + \beta_{13} x_1 x_3 + \beta_{14} x_1 x_4 + \beta_{23} x_2 x_3 + \beta_{24} x_2 x_4 + \beta_{34} x_3 x_4$$

$$(34)$$

According to relevant references and experiences, the values of x_1, x_2, x_3, and x_4 normally lie in some ranges (Eq. (35)). The purpose of optimization is to find appropriate parameters β_{ij} to make sure that the differences between simulated and tested temperatures and thermal growth of the ball screw feed drive system are the smallest.

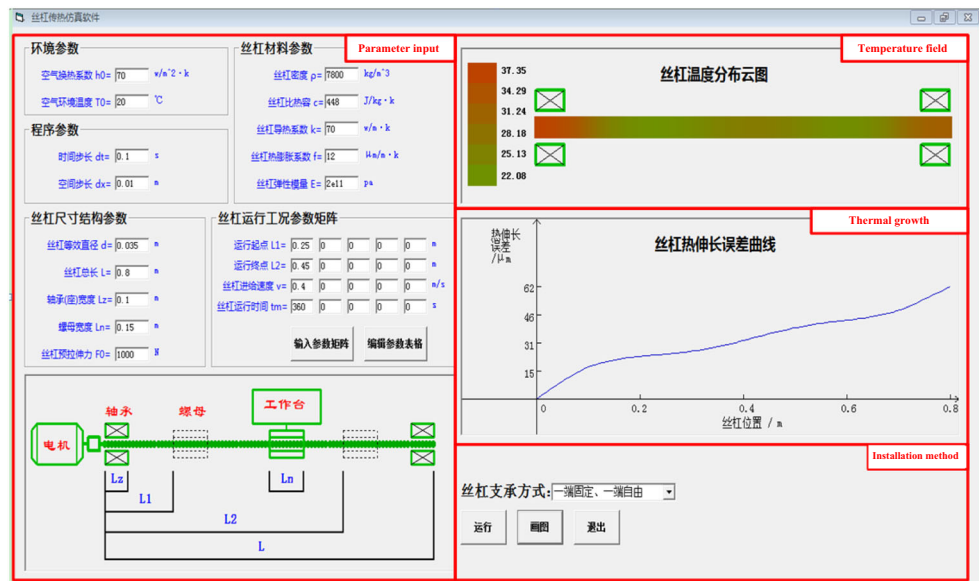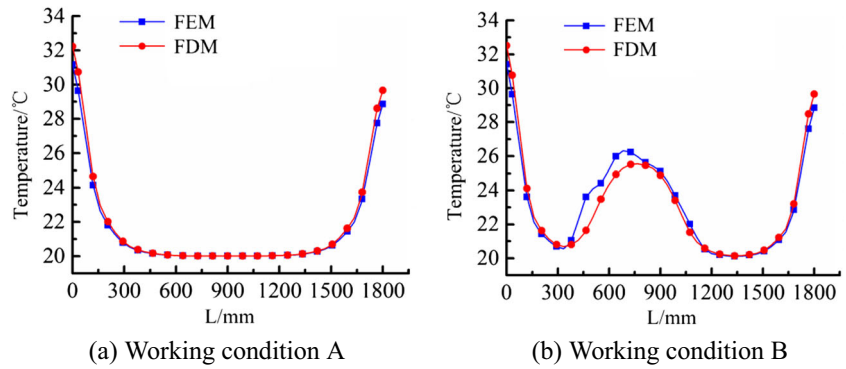**Fig. 8**   Interface of the thermal characteristic analysis software based on FDM

Fig. 9 Simulated temperatures of the ball screw based on FEM and FDM. **a** Working condition A. **b** Working condition B

(a) Working condition A   (b) Working condition B

$$\begin{cases} \min \quad Y(x_1, x_2, \ldots, x_4) \\ s.t. \quad 1500 \leq x_1 \leq 2500; \\ \quad 1000 \leq x_2 \leq 1800 \\ \quad 400 \leq x_3 \leq 1000; \\ \quad 50 \leq x_4 \leq 100; \end{cases} \quad (35)$$

$$\begin{aligned} Y(x_1, x_2, \ldots, x_4) = & \sum_{t=1}^{m} \left[(T_1)_1 - (T_1)'_1 \right]^2 + \left[(T_1)_2 - (T_1)'_2 \right]^2 + \ldots + \left[(T_1)_m - (T_1)'_m \right]^2 \\ & + \sum_{t=1}^{m} \left[(T_2)_1 - (T_2)'_1 \right]^2 + \left[(T_2)_2 - (T_2)'_2 \right]^2 + \ldots + \left[(T_2)_m - (T_2)'_m \right]^2 \\ & + \sum_{t=1}^{m} \left[(T_3)_1 - (T_3)'_1 \right]^2 + \left[(T_3)_2 - (T_3)'_2 \right]^2 + \ldots + \left[(T_3)_m - (T_3)'_m \right]^2 \\ & + \sum_{t=1}^{m} \left[(E)_1 - (E)'_1 \right]^2 + \left[(E)_2 - (E)'_2 \right]^2 + \ldots + \left[(E)_m - (E)'_m \right]^2 \end{aligned}$$

$$(36)$$

where, T_1, T_2, and T_3 are simulated temperatures of the front bearing block, the rear bearing block, and the nut. E is the axial thermal deformation at the rear end of the ball screw feed drive system. T_i, E and T_i', E' ($i = 1, 2, 3$) represent the simulated and tested data, respectively. The test process would be introduced in Section 4. $t_m (m = 1, 2, \ldots, m)$ represents discrete moment.

The variable values before and after optimization are listed in Table 3.

3.3 Thermal characteristic simulation results of the ball screw system under different working conditions

By using MATLAB, the temperature distributions and thermal growths of the ball screw feed drive system under five different working conditions are simulated based on FDM. The flow chart of the thermal characteristic simulation process is shown in Fig. 7 and introduced as follows.

1) Initializing. Setting the initial time and starting position as 0. Supposing the initial temperature of the ball screw feed drive system is 20 °C.
2) According to Eq. (30), the position of the nut at moment t is determined.
3) Based on the nut position $x(t)$ obtained from step 2), heat flux $q(x)$ in Eq. (29) is calculated.
4) Then, $q(x)$ is used to compute the temperature of the element at position x at moment $t + dt$, i.e., $T(x, t + dt)$.
5) Evaluating x. If x is not equal to the length of the ball screw, return to step 3).
6) Evaluating t. If t is equal to the running time, the simulation is finished. If not, return to step 2).

According to the simulation process, a software for analyzing thermal characteristics of the ball screw feed drive system has been developed. The software interface is shown in Fig. 8. In the left, parameters including the structure parameter, physical parameter, and working conditions of the ball screw feed drive system and the environmental parameters are determined and input into the analysis software. After selection of the installation method of the ball screw at the bottom right corner, the temperature field and thermal growth can be computed and showed in the right.

In order to verify the correctness of the analysis, temperatures of the ball screw under some given working conditions (Table 4) are simulated based on FDM and FEM, respectively. The simulation results are compared and shown as follow (Fig. 9).

According to Fig. 9, we know that the simulated temperatures based on FEM and FDM are almost the same. The largest differences between them is about 4%. It verifies the correctness of the analysis based on FDM.

Table 5 Working conditions of the X-axis in a CNC milling machine

No.	1	2	3	4	5
Moving range/mm	0~400	0~800	200~800	600~800	100~600; 300~400; 200~800
Feed rate/m min^{-1}	5.4				5.4
Running time/h	3				0.5; 0.5; 0.5

Fig. 10 Thermal characteristics simulation results of the ball screw feed drive system under working condition 1~4. **a** Temperature. **b** Positioning deviation

(a) Temperature   (b)Positioning deviation
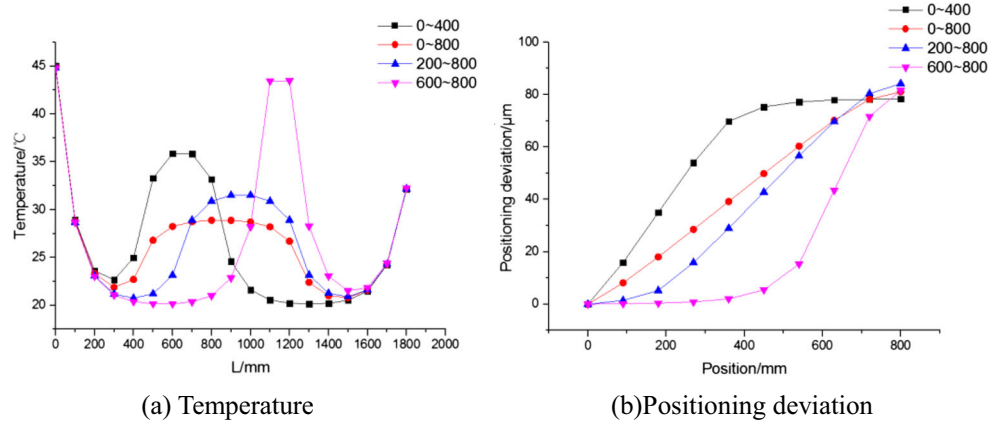
In order to learn more about the thermal characteristics of the X-axis in a CNC milling machine (DK-1200), temperatures and positioning deviations under different working conditions are simulated. The working conditions are illustrated in Table 5. In working condition 1~4 as shown in the table, the nut is moving in different ranges at 5.4 m/min continuously for 3 h. In working condition 5, the ball screw feed system is running from 100 to 300 mm for 0.5 h, then moving from 300 to 400 mm for another half an hour. At last, it moves from 200 to 800 mm for 0.5 h. The feed rate is 5.4 m/min. When the start of the moving range is 0 (Table 5), it means that the coordinate value is 460 mm (Table 1) because there are bearings, bearing house, and other parts at the end of the feed drive system.

The simulation results under working condition 1~4 are shown in Fig. 10.

According to Fig. 10, it can be known that temperatures at both ends of the ball screw and the temperature of the part in which the nut is moving back and forth are higher due to the friction. The high-temperature area of the ball screw shaft is related to the moving range at each working condition. But when the moving range is extended from 400 mm at condition 1 to 800 mm at working

condition 2, the peak temperature of the ball screw feeding system in the moving range is decreased from about 36 to 29 °C. The peak temperature of the ball screw in the moving range at working condition 4 is higher than others, though the moving range is shorter. In addition, the positioning accuracy is deteriorated as the temperature is rising. The position at the front bearing is considered 0, and its positioning deviation is treated as 0 as well, because the ball screw is fixed at the front bearing of which the thermal deformation is assumed as 0. At working conditions 2 and 3, the positioning deviation is almost linear with the coordinate value. The largest positioning deviation of them is about 81 and 82 μm, respectively. At working condition 1, the positioning deviation is becoming larger and larger very fast from position 0 to 400 mm. While at working condition 4, the changing rate of the positioning deviation is higher from position 600 to 800 mm. In other words, the positioning accuracy is decreasing rapidly in the moving range.

Thermal characteristic simulation results under working condition 5 is shown in Fig. 11. The changing trends of the temperature rise, and the positioning deviation are similar with the simulation results obtained under working condition 3.

Fig. 11 Thermal characteristic simulation results of the ball screw feed drive system under working condition 5. **a** Temperature. **b** Positioning deviation
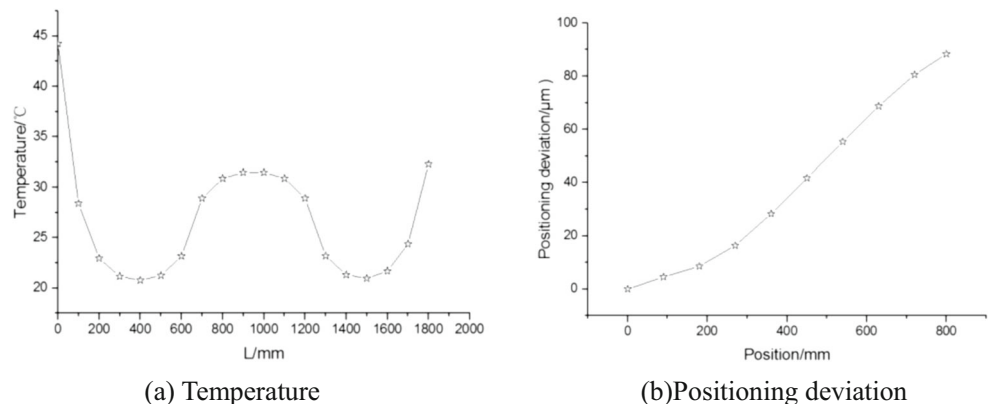

(a) Temperature   (b)Positioning deviation

Table 6 Locations of temperature sensors on a CNC milling machine

No.	1	2	3	4	5	6	7	8
Location	Left bearing	Right bearing	Nut	Motor	Slide	Beam	Environment 1	Environment 2

4 Temperature and thermal deformation testing of prestretching ball screw feed drive

4.1 Experiment set-up

In order to verify the analysis results, a series of tests were conducted on the *X*-axis ball screw feed drive system of a CNC milling machine (DK-1200). The ball screw feed drive system was running under five different working conditions same to the ones listed in Table 5. Temperatures were tested, collected, showed, and saved by eight temperature sensors and a data collection system (CYB-809A). The locations of temperature sensors were illustrated in Table 6 and Fig. 12.

According to ISO230-2 [19] and ISO230-3 [20], the positioning deviations were tested by Renishaw laser interferometer (XL-80). The experimental setup is shown in Fig. 13.

4.2 Testing result

Experimental temperatures of the ball screw feed drive system under working condition 1 to 5 are shown in Fig. 14.

According to the simulation results, it was known that the temperature was rising continuously and rapidly under working condition 1 to 4 when the moving range and feeding rate was unchanged. Under working condition 5, the moving range was various. It had impact on the heat transfer in the ball screw feed drive system and led to anomalous temperature changing. The temperature of the front bearing was higher than the rear bearing as the heat flux of the former was larger according to Table 3. The nut temperature was lower. The temperature rise of the nut was about 3 °C under working condition 1 to 4, and the temperature rise was 2 °C under working condition 5.

According to Fig. 15, it can be seen that the tested positioning deviation curves under different working conditions were close to each other. The positioning accuracy was decreasing continually when the ball screw feed drive was running. After about 3 h, the positioning deviations were basically unchanged under working condition 1 to 4. At the far end of the ball screw (800 mm), the positioning deviation reached to about 88 μm eventually under working condition 2. When the nut was moving at three different ranges (condition 5), it was hard to reach to thermal equilibrium. The positioning deviation was changing all the time, and the largest positioning deviation was more than 80 μm after 1.5 h.

5 Discussion

By comparing the simulation results with the experimental data, we find out that the simulated temperatures at both ends of the ball screw feed drive system are higher than the testing results. This is because temperature sensors are installed on the surface of the bearing house, and the tested temperature is not the real temperature of the bearings. As the experimental temperature data are collected at some certain parts, it is hard to illustrate the temperature distribution all over the ball screw feed drive system. When the ambient temperature changes in the working process, we cannot simulate the thermal characteristics precisely as the environment temperature is considered constant in the simulation program.

The simulated positioning deviations at the far end of the ball screw (at 3 h in working condition 1 to 4 and 1.5 h in working condition 5) are compared with the testing results (Fig. 16).

According to Fig. 16, it can be seen that the simulation results and the experiment data are close to each other. The differences between them lies in the range (− 7 μm,7 μm). However, the changing trends of positioning deviation

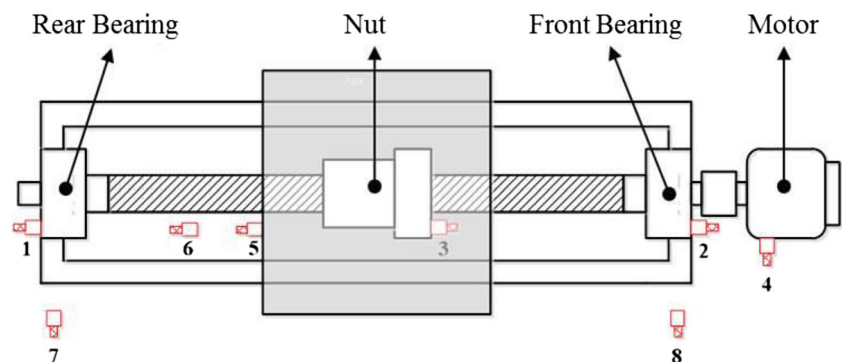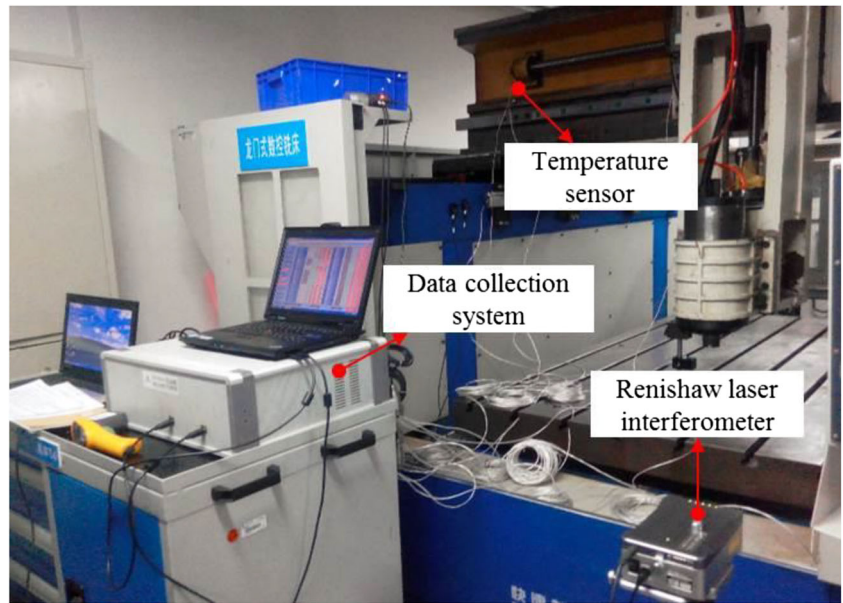**Fig. 12** Locations of temperature sensors

Fig. 13 Experiment set-up on a CNC milling machine

showed in Figs. 10, 11 and 15 are not the same. The tested positioning deviation curves are close to linearity at the end of

experiments. By contrast, the simulated positioning deviations are clearly nonlinear with the position. It may be because that

Fig. 14 Temperature testing results of the ball screw feed drive system under different working conditions. **a** Working condition 1. **b** Working condition 2. **c** Working condition 3. **d** Working condition 4. **e** Working condition 5

(a) Working condition 1

(b) Working condition 2

(c) Working condition 3

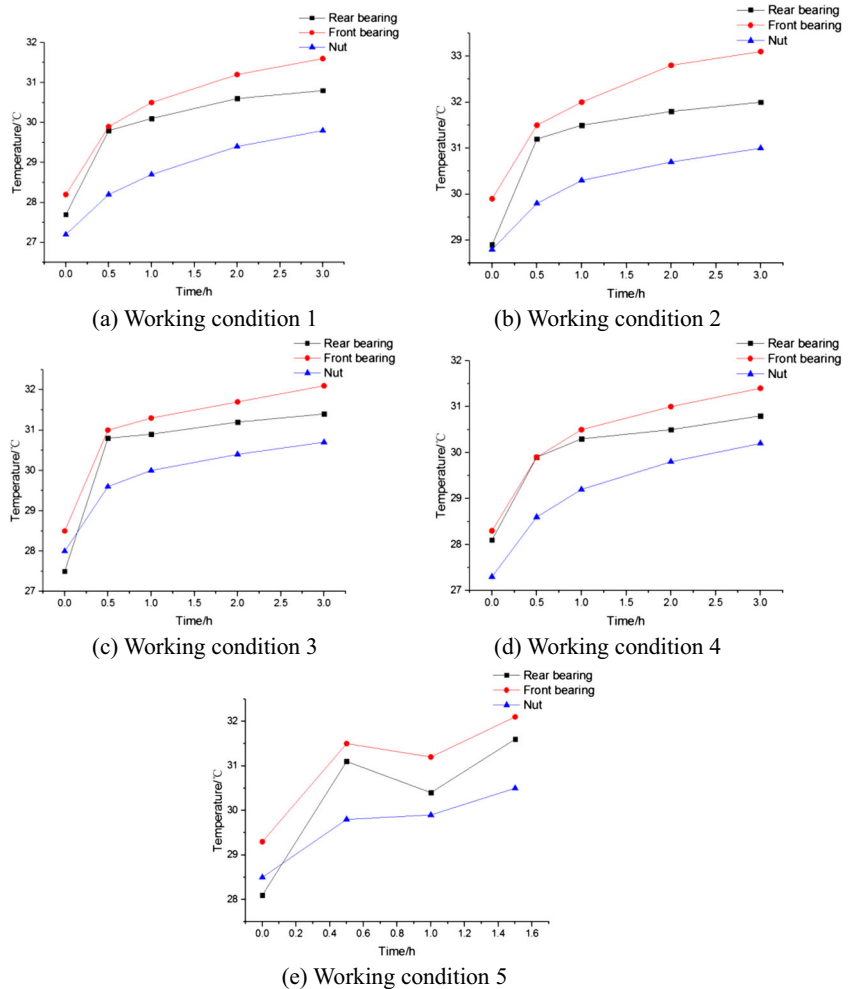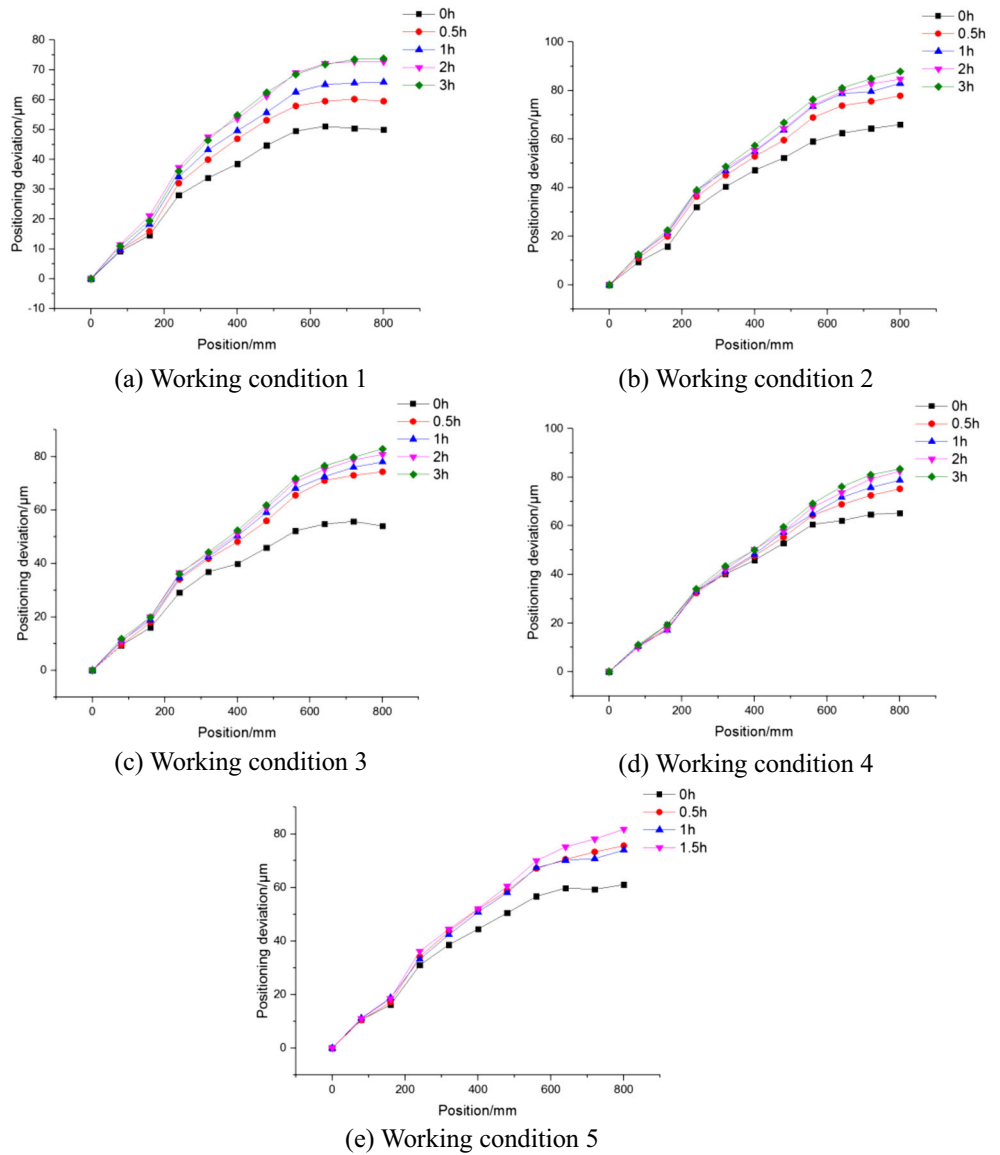(d) Working condition 4

(e) Working condition 5

Fig. 15 Experimental positioning deviation under different working conditions. **a** Working condition 1. **b** Working condition 2. **c** Working condition 3. **d** Working condition 4. **e** Working condition 5

(a) Working condition 1

(b) Working condition 2

(c) Working condition 3

(d) Working condition 4

(e) Working condition 5

Fig. 16 Comparison between the simulation and testing results

in simulation, the structure of the feed drive system is simplified, and the thermal resistances are neglected.

6 Conclusion

In this paper, thermal characteristics of the ball screw feed drive system under various working conditions were studied based on finite difference method. In order to improve the accuracy of the analysis, the nut was considered a moving heat source, and the boundary conditions were optimized based on the response surface methodology. By comparing, we found out that the errors between the simulated positioning deviations at the far end of the ball screw and the experimental data were acceptable small. Based on the finite difference analysis process in this paper, an analysis software has been developed. It provided an easy, reliable, and costless way to
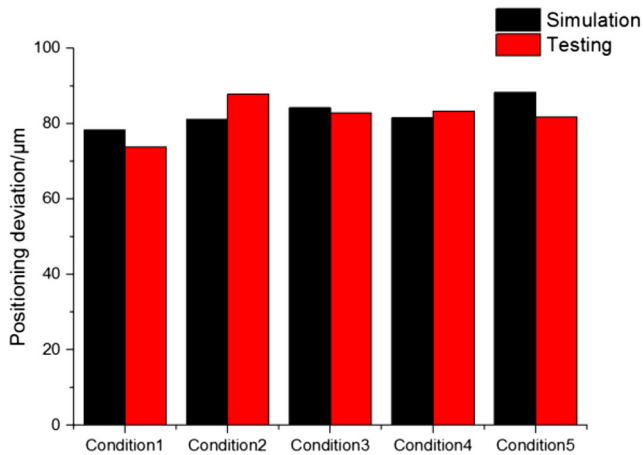
know the thermal characteristics of the ball screw feed drive system by using the proposed method, and the simulation results could help engineers to optimize the structure or adjust machining program.

References

1. Horejs, O (2007) Thermo-mechanical model of ball screw with non-steady heat sources. in International Conference on Thermal Issues in Emerging Technologies: Theory & Application.

2. Li TJ, Zhao C-Y, Zhang Y-M (2018) Adaptive real-time model on thermal error of ball screw feed drive systems of CNC machine tools. Int J Adv Manuf Technol 94(9–12):3853–3861

3. Kim SK, Cho DW (1997) Real-time estimation of temperature distribution in a ball-screw system. Int J Mach Tool Manu 37(4):451–464

4. Liu K, Liu Y, Sun M, Wu Y, Zhu T (2016) Comprehensive thermal compensation of the servo axes of CNC machine tools. Int J Adv Manuf Technol 85(9–12):2715–2728

5. Li B, Tian X, Zhang M (2019) Thermal error modeling of machine tool spindle based on the improved algorithm optimized BP neural network. Int J Adv Manuf Technol 105:1497–1505

6. Liu D-S, Lin P-C, Lin J-J, Wang CR, Shiau TN (2019) Effect of environmental temperature on dynamic behavior of an adjustable preload double-nut ball screw. Int J Adv Manuf Technol 101(9–12): 2761–2770

7. Li R, Lin W, Zhang J, Chen Z, Li C, Shuang Q (2018) Research on thermal deformation of feed system for high-speed vertical machining center. Procedia Comput Sci 131:469–476

8. Min X, Jiang S (2011) A thermal model of a ball screw feed drive system for a machine tool. P I Mech Eng C-J Mec 225(1):186–193

9. Oyanguren A, Larrañaga J, Ulacia I (2018) Thermo-mechanical modelling of ball screw preload force variation in different working conditions. Int J Adv Manuf Technol 2:1–17

10. Li TJ, Zhao CY, Zhang YM (2018) Adaptive real-time model on thermal error of ball screw feed drive systems of CNC machine tools. Int J Adv Manuf Technol 94(9–12):3853–3861

11. Wu CH, Kung YT (2003) Thermal analysis for the feed drive system of a CNC machine center. Int J Mach Tool Manu 43(15): 1521–1528

12. Xu ZZ, Choi C, Liang LJ, Li DY, Lyu SK (2015) Study on a novel thermal error compensation system for high-precision ball screw feed drive (1st report: model, calculation and simulation). Int J Precis Eng Manuf 16(9):2005–2011

13. Shi H, Zhang D, Yang J, Ma C, Mei X, Guo G (2016) Experiment-based thermal error modeling method for dual ball screw feed system of precision machine tool. Int J Adv Manuf Technol 82(9–12): 1693–1705

14. Shi H, Ma C, Yang J, Zhao L, Mei X, Guo G (2015) Investigation into effect of thermal expansion on thermally induced error of ball screw feed drive system of precision machine tools. Int J Mach Tool Manu 97:60–71

15. Yang J, Mei X, Feng B, Zhao L, Ma C, Shi H (2015) Experiments and simulation of thermal behaviors of the dual-drive servo feed system. Chin J Mech Eng-En 28(1):76–87

16. Harris TA (1991) Rolling bearing analysis. Wiley, New York

17. Lienhard JH, Lienhard J (2000) A heat transfer textbook. Phlogiston Press, Cambridge, Massachusetts

18. Montgomery D (2007) Design and analysis of experiments. 6th Edition, John Wiley & Sons, New York

19. ISO (2006) 230-2:Test code for machine tools—part 2: determination of accuracy and repeatability of positioning numerically controlled axes.

20. ISO (2007) 230-3: Test code for machine tools—part 3: determination of thermal effects.